

Raman excitation profiles for the (n_1, n_2) assignment in carbon nanotubes

H. Telg*, J. Maultzsch*, S. Reich†, F. Hennrich** and C. Thomsen*

**Institut für Festkörperphysik, TU Berlin, Hardenbergstr. 36, 10623 Berlin, Germany*

†*Department of Engineering, University of Cambridge, United Kingdom*

***Institut für Nanotechnologie, Forschungszentrum Karlsruhe, 76021 Karlsruhe, Germany*

Abstract. The assignment of the chiral indices n_1 and n_2 in semiconducting and metallic nanotubes was performed comparing resonance Raman profiles and transition energies in a 3rd-order Kataura plot. We find several complete branches in the Kataura plot and are able to assign the resonance peaks to n_1 and n_2 without prior assumptions about the constant of proportionality between the radial-breathing mode frequency ω_{RBM} and the inverse diameter of the tube. We point out systematic differences in the transition energies and intensities in +1 and -1 nanotube families.

Ever since the discovery of how to keep isolated nanotubes from rebundeling in solution, it has become a realistic goal to identify the chirality of a nanotube by spectroscopic methods. Wrapping the nanotubes with SDS, Bachilo *et al.* [1] found that the luminescence from semiconducting nanotubes was large and not quenched by the presence of metallic tubes. They were able to map out luminescence energies of a sample as a function of laser-excitation energy and found a series of peaks presumably originating from different chirality nanotubes. There were, however, several possibilities for matching the experimental transition energies E_{11} and E_{22} to the calculated energies.[2] To remove these ambiguities the authors had to define an anchoring element from which the chirality assignment of all other detected nanotubes followed. This anchoring element was found by minimizing the least-square error of detected RBM frequencies for several different constants in the well-known inverse-diameter dependence of nanotubes.

In this paper we study the excitation-energy dependence of the Raman intensity of the radial breathing mode. The resonance maxima yield the transition energies $E_{ii}^{S,M}$, the frequency of the RBM peak we take to be proportional to the inverse diameter of the tube (plus a constant), but we do not make *a priori* assumptions about the proportionality constant as is usually done. Instead, plotting the resonance maxima of the radial breathing mode *versus* $1/\omega_{\text{RBM}}$, we are able to resolve the individual branches of the radial breathing mode in a 3rd-order Kataura plot. The ambiguities in the assignment of the Raman peaks arising from the closely spaced ω_{RBM} are removed and a straightforward assignment of the RBM-peaks to chiral indices n_1 and n_2 follows. Our assignment agrees with the one given by Bachilo *et al.* [1], and partly also with the one of Strano *et al.* [3] but is different from many others. Different from luminescence measurements we also find metallic tubes and several zig-zag tubes.

From our results we can derive an independent value for the proportionality constant in the frequency–inverse-diameter relationship, generally taken to be between 200 and

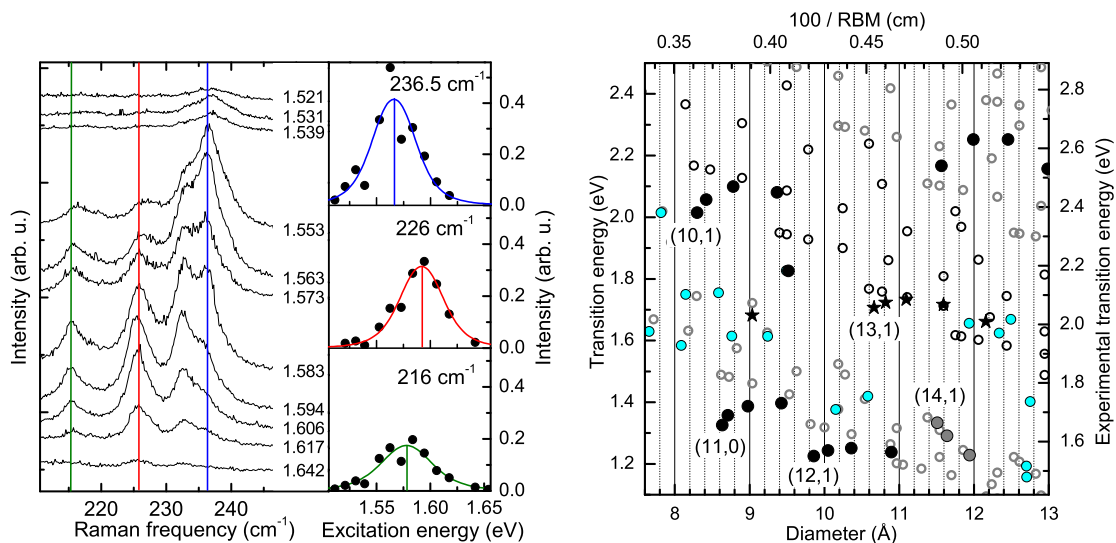


FIGURE 1. *left:* Resonance Raman spectra of the radial breathing mode excited with various laser energies of a dye laser as indicated. *right:* Kataura plot with the transition energies calculated in the 3rd-order tight-binding approximation,[2] vs theoretical diameter d (left and bottom axes, open symbols). Right and top axes refer to experimental values (black circles—strong, stars—medium, light gray—weak). The chirality of the tube with the smallest d within a branch is indicated just below or above that tube.

250 cm⁻¹ nm [4] and heavily debated in the literature. The importance of this relationship lies in that it gives practical information about the diameter and even the chirality of an observed nanotube, both essential for most applications of carbon nanotubes. In contrast to its general importance, however, it was never established independently from experiment. There are many calculations putting the constant between 230-235 cm⁻¹, at least for the larger diameters; see, *e.g.*, Ref. [5] for an overview.

In Fig. 1, *left*, we show one of the resonance profiles of several nanotubes with nearby resonance maxima. The largest intensity is seen to move through the peaks forming what looks similar to a laola wave.[6] There are several such laola-type resonances when exciting the nanotubes with different laser lines, each occurring over a fairly narrow energy and ω_{RBM} range. As we will see, each laola-series of resonances corresponds to a particular branch in the Kataura plot of transition energies *versus* diameter. Within each such a branch, there is a fixed relationship between the indices: n_1 decreases by one and n_2 increases by 2, going from smaller to larger diameters as long as $n_1 > n_2$. The tube with a smallest diameter in a branch is thus always a zig-zag or near-zig-zag tube.

We are now able to plot the transition energies obtained from the resonance profiles *versus* the inverse radial breathing mode frequency, both purely experimental values. In order to make the experiment (right and top axes in Fig. 1, *right*) match theory (left and bottom axes) in this plot, we stretch and/or shift the axes in the plot. For the x -axis this means varying the proportionality constant in the frequency–inverse-diameter relationship and introducing a constant offset. For the y -axis this adjusts the tight-binding energies to the experimental transition energies. We perform this transformation until we get a match between experiment and theory. Our stringent criterion is that in the vertical

TABLE 1. Chiral indices and RBM-frequencies ($\pm 0.5 \text{ cm}^{-1}$) as determined from a comparison to several branches of the 3rd-order Kataura plot, see Fig. 1. The modes are grouped into branches and sorted in order of increasing smallest diameter d in a branch. (d is calculated from n_1 and n_2 with a graphite lattice constant of $a_0 = 2.461 \text{ \AA}$.) Also given is the family $v = (n_1 - n_2) \bmod 3$; [7] $v = 0$ corresponds to metallic nanotubes. The resonance maxima E_{22}^S and E_{11}^M are accurate to ± 3 (3 digits) or ± 30 meV (2 digits).

family v	chirality	$\omega_{\text{RBM}}[\text{cm}^{-1}]$	$d[\text{\AA}]$	strength	$E_{22}^S[\text{eV}]$	$E_{11}^M[\text{eV}]$
0	10, 1	276.3	8.25	strong		2.38
	9, 3	272.7	8.47	strong		2.43
	8, 5	262.7	8.90	strong		2.47
	7, 7	247.8	9.50	strong		2.45
-1	11, 0	266.7	8.62	strong	1.657	
	10, 2	264.6	8.72	strong	1.690	
	9, 4	257.5	9.03	strong	1.72	
	8, 6	246.4	9.53	strong	1.73	
-1	12, 1	236.4	9.82	strong	1.551	
	11, 3	232.6	10.00	strong	1.570	
	10, 5	226.1	10.36	strong	1.578	
	9, 7	216.0	10.88	strong	1.564	
0	13, 1	220.3	10.60	medium		2.057
	12, 3	217.4	10.77	medium		2.075
	11, 5	212.4	11.11	medium		2.084
	10, 7	204.0	11.59	medium		2.067
	9, 9	195.3	12.21	medium		2.01
+1	14, 1	205.4	11.38	weak	1.667	
	13, 3	203.3	11.54	weak	1.617	
	12, 5	198.5	11.85	weak	1.554	
	11, 7	–	12.31	–	–	
	10, 9	–	12.09	–	–	

direction there is a full correspondence between experiment and theory implying that all chiralities theoretically possible have actually been detected. Note that some chiralities give rather close diameters and hence closely lying peaks, *e.g.*, $d[(11, 0)] = 8.6$ and $d[(10, 2)] = 8.7 \text{ \AA}$ whereas the next tube in the same branch is at a larger separation, $d[(9, 4)] = 9.0 \text{ \AA}$. For the four branches with the smallest tubes (10,1), (11,0), (12,1), and (13,1) we observed all possible nanotubes, the irregularities in the diameter distances were observed as well and put our assignment on firm grounds, see Table 1.

The requirement to find *all* experimental peaks in a given branch leads to a unique relationship between inverse diameter and ω_{RBM} . This makes clear the advantage of resonant Raman over luminescence spectroscopy where the zig-zag tubes were not observed, and hence the horizontal alignment in the Kataura plot could not be performed uniquely, consequently leading to ambiguities in the chirality assignment and/or somewhat far-fetched assumption about the chirality distributions in a sample.[1]

In Table 1 we summarize the radial breathing mode frequency and the chirality assignment as obtained from our experiment and as plotted in Fig. 1. We stress that the assignment is actually independent of the actual transition energies and their systematic

deviations from the 3rd-order transition energies, but relies on the completeness of all possible chiralities within several branches of the Kataura plot. Our assignment agrees with that given by Bachilo *et al.*[1], but disagrees with several others in the literature.

As regards to the vertical axis in Fig. 1, *right*, we observe the following for tubes of the -1 and 0 families: Shrinking the vertical axis aligns well the nanotubes with near-armchair direction chiralities but leaves a systematically increasing deviation between experiment and theory when moving towards the zig-zag direction within a given branch. In other words, the experimental points within a Kataura branch curve away from the $1/d$ center of gravity of the transition energies more strongly than the calculated values. This systematic difference, also observed in luminescence spectroscopy, [1, 4] is apparently due to a chirality-dependent effect and currently under investigation,[8] together with a systematic dependence of the Raman intensity on chiral angle within a branch.[9] A second observation regarding the intensities of semiconducting tubes is at place: The lower branches in the Kataura plot are systematically much stronger experimentally than the upper ones. In terms of the chiralities this distinction translates into families with $(n_1 - n_2) \bmod 3 = -1$ (lower branch) having generally larger intensities than those with $+1$ (upper branch). This asymmetric behavior has been shown to originate from band renormalization effects [10] as predicted by Kane and Mele.[11] and a dependence of the RBM matrix element on the nanotube family.[9].

In conclusion, we reported an assignment of RBM frequencies to carbon nanotube chiralities based on resonance Raman spectroscopy. The assignment is independent of prior assumptions about the frequency–diameter relationship; instead, including also RBM frequencies not shown here, this relationship is experimentally determined as [12]

$$\omega_{\text{RBM}} = \frac{(216 \pm 2) \text{ cm}^{-1} \text{ nm}}{d} + (17 \pm 2) \text{ cm}^{-1} \quad (1)$$

We also pointed out systematic differences of the measured and calculated transition energies and of the Raman intensities within a branch or a family of the Kataura plot.

We acknowledge support by the Deutsche Forschungsgemeinschaft under grant number Th 662/8-2. SR was supported by the Oppenheimer Fund and Newnham College.

REFERENCES

1. S.M. Bachilo, M.S. Strano, C. Kittrell, R.H. Hauge, R.E. Smalley, and R.B. Weisman, *Science* **298**, 2361 (2002)
2. S. Reich, J. Maultzsch, C. Thomsen, and P. Ordejón, *Phys. Rev. B* **66**, 035 412 (2002)
3. M.S. Strano *et al.*, *Nano Lett.* **3**, 1091 (2003)
4. S. Reich, C. Thomsen and J. Maultzsch, *Carbon Nanotubes: Basic Concepts and Physical Properties* (Wiley-VCH, Weinheim, 2004)
5. J. Kürti, V. Zólyomi, M. Kertesz, and G. Su, *New Journal of Physics* **5**, 125 (2003)
6. I. Farkas, D. Helbing, and T. Vicsek, *Nature* **419**, 131 (2002)
7. S. Reich and C. Thomsen, *Phys. Rev. B* **62**, 4273 (2002)
8. S. Reich *et al.*, to be published
9. M. Machón, S. Reich, J. Maultzsch, P. Ordejón, and C. Thomsen, to be published
10. S. Reich, M. Dworzak, A. Hoffmann, M.S. Strano, and C. Thomsen, to be published
11. C.L. Kane and E.J. Mele, *Phys. Rev. Lett.* **90**, 207 401 (2003), and cond-mat 0403153 (2004)
12. H. Telg, J. Maultzsch, S. Reich, F. Hennrich, and C. Thomsen, to be published